Results in Nonlinear Analysis 7 (2024) No. 1, 89–109
https://doi.org/10.31838/rna/2024.07.01.010
Available online at www.nonlinear-analysis.com

Results in Nonlinear Analysis
ISSN 2636-7556

Peer Reviewed Scientific Journal

Modeling the dynamics of a marine system using the fractional order approach to assess its susceptibility to global warming

R.N. Premakumari[1], Chandrali Baishya[1], Mohammad Sajid[2,*], Manisha Krishna Naik[1]

[1]Department of Studies and Research in Mathematics, Tumkur University, Tumkur-572103, Karnataka, India; [2]Department of Mechanical Engineering, College of Engineering, Qassim University, Buraydah-51452, Saudi Arabia.

Abstract

In the marine ecosystem, phytoplankton plays a vital role as the primary supplier of oxygen, contributing to 50% of the total oxygen production. Not only does it serve as a significant source of food for other species, but it also sustains life in the ocean. However, the rising ocean temperatures caused by global warming have severely hindered the ability of phytoplankton to generate oxygen. Furthermore, fishes are crucial consumers of oxygen within the marine ecosystem. This research paper presents a model that intricately connects the dynamics of oxygen, phytoplankton, zooplankton, and fish using the Caputo fractional derivative. The model aims to examine the impact of global warming on the collective dynamics by considering the relationship between the rate of oxygen generation, temperature, and time. The paper establishes the existence and uniqueness of solutions and also analyzes the stability of equilibrium points. Numerical simulations are conducted to demonstrate the impact of fractional derivatives and global warming on oxygen depletion and species extinction.

Key words and phrases. Caputo fractional derivatives, simulation, oxygen, plankton, fish, global warming, numerical results

Mathematics Subject Classification (2010): 2020 MSC: 26A33, 37N25, 70K20, 92B05, 92D40

1. Introduction

Email addresses: premakumarirn12@gmail.com (R.N. Premakumari); baishyachandrali@gmail.com (Chandrali Baishya); msajd@qu.edu.sa (Mohammad Sajid); manishakn06@gmail.com (Manisha Krishna Naik)
*Corresponding Author

Received October 9, 2023; Accepted November 11, 2023; Online December 29, 2023

Global warming is a topic of significant debate due to its widespread impact on the world. It leads to several issues such as floods, droughts, and rising sea levels. The marine environment is also greatly affected by global warming, which is of particular concern as the oceans cover almost two-thirds of the earth's surface and are considered a significant contributor to climate change. Rising temperatures caused by carbon dioxide emissions are the primary cause of global warming. The effect of greenhouse gases has led to a more rapid change in the climate than during the pre-industrial era. Carbon dioxide, in particular, plays a crucial role in the acceleration of global warming. Increased greenhouse gas emissions boost the earth's surface temperature, contributing to climate change, which is hazardous to the environment of marine species. The book [1] delves into numerous chapters discussing pivotal aspects of plankton dynamics, including topics such as plankton patches, spatial structures in phytoplankton populations analyzed through spectral analysis, small-scale distribution of plankton, and the biological ramifications of vertical-horizontal interactions. Meanwhile, the book [2] provides an overview of diverse mathematical models concerning diffusion within an ecological framework. Book [3] focuses on exploring the ecological implications resulting from recent climate change. Moreover, in [4], the exploration extends beyond the traditional Turing scenario, demonstrating how mathematical models and numerical simulations shed light on spatiotemporal patterns in ecology and epidemiology. A broad spectrum of subjects related to plankton ecology is encompassed within book [5]. Finally, book [6] compares seafloor-derived planktonic foraminifera communities of the pre-industrial era with those from sediment-trap time series, revealing differences in the Anthropocene communities of this globally distributed zooplankton group compared to their original, undisturbed pre-industrial state.

The United Nations Climate Change Conference was held in Glasgow, UK in 2021, and its primary objective was to decrease greenhouse gas emissions, particularly carbon dioxide emissions. The conference established a goal of reducing emissions by 45% by 2030, based on 2010 levels, and achieving net-zero emissions by the middle of the century. Although plankton is a tiny organism that lives in freshwater and seawater, it plays a vital role in regulating global warming. Phytoplankton and zooplankton are the two types of plankton. Phytoplankton is an organism that can produce its sustenance from water, light, carbon dioxide, or other important ingredients, and zooplankton is a little animal that swims in water and floats with the currents, and it is food, carbon, and energy-dependent on other plants and animals. Phytoplankton and zooplankton have a tight relationship. Zooplankton feeds on phytoplankton in the aquatic environment. Sekerci and Petrovskii developed a novel model that evaluated climatic change by linking oxygen, phytoplankton, and zooplankton [7]. Phytoplankton contributes a considerable amount of oxygen to the atmosphere, accounting for 50 to 70% of it. When enough light is available, phytoplankton, like plants, creates oxygen through photosynthesis. This oxygen, which initially reaches water before entering the atmosphere via the sea surface, is a massive contribution of oxygen to the atmosphere.

Over the years, several groundbreaking research on the marine ecosystem has been done. Some of the biological models of phytoplankton-zooplankton interaction can be found in [8–11]. Zhang and Wang conducted research on the interaction model between nutrient-phytoplankton-zooplankton-fish in their study [12]. Meanwhile, Mishra studied the depletion of dissolved oxygen in a lake caused by submerged macrophytes in their work while considering constant water flow and nutrient availability [13]. Furthermore, Ozarsian and colleagues examined the impact of global warming on the relationship between oxygen and plankton in their research. They found that rising temperatures due to global warming have a significant impact on aquatic environments, leading to a decrease in oxygen levels that can cause the death of phytoplankton species [14].

The development of fractional calculus has opened up new possibilities for mathematical modeling, as explored by researchers [15, 16]. Fractional derivatives (FDs), such as the Caputo, Caputo-Fabrizio, and Atangana-Baleanu derivatives, have been used to re-examine classical problems with impressive results, as demonstrated by Kumar et al. [17], Gao et al. [18]. The authors in [19] have employed a modified SIR model, utilizing fractional derivatives, to analyze worm transmission within a wireless sensor network. [20], investigates the dynamics of a fractional epidemiological model encompassing disease infection in both populations. Hammouch et al. presented the synchronization of a variable-order fractional chaotic system in their work [21]. In [22, 23], new solution techniques for solving fractional differential equations are proposed by the authors. Dubey et al. explored the fractional blood glucose-insulin minimal model [24]. Furthermore, [25] discusses chaos controllability in fractional-order systems using an active dual combination hybrid synchronization strategy. Researchers' interest in fractional derivatives is evident in various works, such as option pricing models [26], a fractional-order epidemic model with a nonlinear incidence function [27], and a COVID-19 infection system considering leaky vaccination efficacy [28]. In [29], authors have investigated tumar growth model in the frame of fractal Caputo-Fabrizio fractional derivative. These works collectively demonstrate the keen interest of researchers in the application of fractional derivatives across diverse fields.

The application of fractional calculus to marine dynamics has also been explored, such as in the work of Ghanbari and Gomez-Aguilar in [30] and Ghanbari and Salih in [31], who investigated fractional predator-prey models. Shi et al. [32] analyzed a nutrient-phytoplankton-toxic phytoplankton-zooplankton model with time delay, while Veeresha and Akinyemi [33] studied a phytoplankton-toxic phytoplankton-zooplankton system using the q-homotopy analysis transform method. Javidi et al. [34] examined a time-fractional order toxic-phytoplankton-phytoplankton-zooplankton system. Significant contributions in the fractional domain to the study of marine species can also be found in [35, 36]. The effects of climate change on the marine ecosystem have been studied from a fractional calculus perspective by Eze and Oyesanya in [37, 38], who examined the effects of climate change on the Pacific Ocean, and by Din et al. [39], who investigated the behavior of climate change in a mathematical formulation using the interaction between oxygen, phytoplankton, and zooplankton.

This study examines the effects of global warming on the oxygen-phytoplankton-zooplankton-fish system, utilizing the Caputo fractional order derivative to incorporate the impact of temperature changes on the system's dynamics. Novelty of the present work can be highlighted in terms of the study of three interconnected marine species under the imapct of oxygen supply and global warming. Even though oxygen-phytoplankton-zooplankton dynamics is studied with global warming influence, fishes being a major contributors to arine environment, their inclusion in the current model adds new observations to this dynamics. The study reveals that an increase in ocean surface temperature due to global warming significantly affects the rate of oxygen production by phytoplankton, leading to oxygen depletion and the extinction of plankton species. However, fish populations can continue to thrive even in the presence of oxygen depletion. We introduce some basic definitions and theorems related to the fractional order derivative in Section 2, followed by model formulations with classical and fractional order derivative descriptions in Section 3. Sections 4 through 5 discuss the existence of solutions, boundedness, and equilibrium points. The numerical simulations and the results are presented in Section 6, and the conclusion of the article is presented in Section 7.

Some necessary definitions and theorems

The Caputo FD has been used in the current work. We've included some definitions for Caputo FDs, which are employed in the paper's primary conclusion.

Definition 2.1. [40] (Caputo FD) Assume that $h(t)$ is an integrable and continuously differentiable function in $[t_0, \bar{\tau}]$. Then, the Caputo FD of order $0 < \alpha < 1$ for a function $h(t)$ is defined as:

$$D_{t_0}^{\alpha} h(t) = \frac{1}{\Gamma(1-\alpha)} \int_{t_0}^{t} (t-\tau)^{-\alpha} h'(\tau) d\tau, \tag{1}$$

where $\Gamma(\cdot)$ denotes Gamma function.

Definition 2.2. The Riemann-Liouville fractional order integral operator is defined as [40]

$$J_v^{\alpha} f(v) = \frac{1}{\Gamma(\alpha)} \int_{t_0}^{v} \frac{f(t)}{(v-t)^{1-\alpha}} dt, \alpha > 0,$$

$$J^0 f(v) = f(v).$$

Lemma 1. [41] Consider the system:

$$D_{t_0}^{\alpha} x(t) = h(t,x), t > t_0, x(t_0) = x_0.$$

Here, $0 < \alpha \leq 1$ and $h : [t_0, \infty) \times \Omega \rightarrow \mathbb{R}^n$, $\Omega \in \mathbb{R}^n$. If $h(t, x)$ satisfies the locally Lipschitz conditions concerning to x, the system has a unique solution on $[t_0, \infty) \times \Omega$.

Lemma 2. [40] let $h(t)$ be a continuous function on $[t_0,+\infty)$ and satisfying

$${}_{t_0}^{C} D_t^{\alpha} h(t) \leq -\lambda h(t) + \iota, h(t_0) = f_{t_0},$$

where $0 < \alpha \leq 1$, $(\lambda , \iota) \in \mathbb{R}_2$ and $\lambda \neq 0$ and $t_0 \geq 0$ is the initial time. Then,

$$h(t) \leq \left(h(t_0) - \frac{\iota}{\lambda} \right) E_{\alpha}[-\lambda(t-t_0)^{\alpha}] + \frac{\iota}{\lambda}.$$

Theorem 2.1. [42] Consider the system of n-dimensional fractional differential equation:

$$D_{t_0}^{\alpha} g(t) = Ag(t), 0 < \alpha < 1, \tag{2}$$

where A is an $n \times n$ matrix of constants .

1. The stability of the system's solution, denoted as $g(t)$, is determined by the eigenvalues of the system's matrix A. Specifically, $g(t)$ is stable if and only if the eigenvalues satisfy the condition $\left|\arg(\lambda_j)\right| \geq \frac{\alpha\pi}{2}$, where α is a given constant. Additionally, any eigenvalue with $\left|arg(\lambda_j)\right| = \frac{\alpha\pi}{2}$ must have the same number of linearly independent eigenvectors as its algebraic multiplicity.

2. On the other hand, the solution $g(t)$ is said to be asymptotically stable if all the eigenvalues λ_j of the matrix A satisfy the condition $\left|arg(\lambda_j)\right| > \frac{\alpha\pi}{2}$, where α is a constant. This condition guarantees that the solution approaches zero as t tends to infinity.

3. Model formulation

The marine ecosystem is a dynamic and intricate network that comprises a vast array of living and non-living components, such as different species, organic and inorganic substances, and chemical compounds. Building on the research of Sekerci and Petrovskii [7] and Ozarslan and Sekerci [14], we have developed a model to investigate the interactions among dissolved oxygen, phytoplankton, zooplankton, and fish populations. The model's formulation is as follows:

$$\frac{dW}{d\tau} = \hat{T}\left(1 - \frac{W}{W + \hat{a}_1}\right)X - \frac{\hat{\delta}_1 XW}{W + \hat{a}_2} - \frac{\hat{\delta}_2 YW}{W + \hat{a}_3} - \frac{\hat{\delta}_3 ZW}{W + \hat{a}_4} - mW,$$

$$\begin{aligned}
\frac{dX}{d\tau} &= \left(\frac{\hat{G}W}{W+\hat{a}_5} - \rho X\right)X - \frac{\beta_1 XY}{X+\hat{b}_1} - \frac{\beta_2 XZ}{X+\hat{b}_2} - \hat{\sigma}_1 X,\\
\frac{dY}{d\tau} &= \left(\frac{\hat{v}_1 W^2}{W^2+\hat{a}_6^2}\right)\left(\frac{\beta_1 XY}{X+\hat{b}_1}\right) - \frac{\hat{\zeta}_1 YZ}{Y+\hat{c}} - \hat{\sigma}_2 y,\\
\frac{dZ}{d\tau} &= \left(\frac{\hat{v}_2 W^2}{W^2+\hat{a}_7^2}\right)\left(\frac{\beta_2 XZ}{X+\hat{b}_2}\right) + \frac{\hat{\zeta}_2 YZ}{Y+\hat{c}} - \hat{\sigma}_3 Z.
\end{aligned} \tag{3}$$

The meaning of the parameters are as follows:
W is the concentration of oxygen.
X, Y and Z are the densities of phytoplankton, zooplankton and fish.
$\hat{T}$ represents the oxygen produced within the phytoplankton cells.
$\hat{\delta}_1$, $\hat{\delta}_2$ & $\hat{\delta}_3$ are the inhalation coefficients of phytoplankton, zooplankton and fish respectively.
$\hat{G}$ is maximum growth rate of phytoplankton.
$\hat{a}_1$ is the half-saturation constant of oxygen produced by the phytoplankton.
$\hat{a}_2$, $\hat{a}_3$ & $\hat{a}_4$ are half-saturation constants of inhalation of phytoplankton, zooplankton and fish respectively.
$\hat{a}_5$ is the half-saturation constant of phytoplankton growth.
$\hat{a}_6$ & $\hat{a}_7$ are the half-saturation constant of feeding efficiency of zooplankton and fish respectively.
m is the natural depletion rate of oxygen.
ρ represents the intraspecific conflict coefficient of phytoplankton species.
β_1 & β_2 are maximum predation rate of zooplankton and fish respectively.
$\hat{v}_1$ & $\hat{v}_2$ are the feeding efficiency of zooplankton and fish respectively.
$\hat{\zeta}_1$ is the maximum predation rate of fish.
$\hat{\zeta}_2$ is the conversion rate of zooplankton to fish population.
$\hat{b}_1$ & $\hat{b}_2$ are the half-saturation constants of phytoplankton density.
$\hat{c}$ is the half-saturation constant of zooplankton density.
$\hat{\sigma}_1$, $\hat{\sigma}_2$ & $\hat{\sigma}_3$ are the natural death rate of phytoplankton, zooplankton, and fish respectively.

All the parameters are taken on non-negative. To reduce the number of parameters in the system (3), we consider the dimensionless form of variables,

$$t = m\tau,\ w = \frac{W}{a_1},\ x = \frac{\rho X}{m},\ y = \frac{\beta_1 Y}{m},\ z = \frac{\beta_2 Z}{m}.$$

As a result, the new dimensionless parameters can be seen as:

$$G = \frac{\hat{G}}{m}, T = \frac{\hat{T}}{\hat{a}_1\rho}, \delta_1 = \frac{\hat{\delta}_1 m}{\hat{a}_1\rho}, \delta_2 = \frac{\hat{\delta}_2 m}{\beta_1\hat{a}_1}, \delta_3 = \frac{\hat{\delta}_3 m}{\beta_2\hat{a}_1}, c = \frac{\beta_1\hat{c}}{m}, \nu_1 = \frac{\beta_1\hat{\nu}_1}{m}, \nu_2 = \frac{\beta_2\hat{\nu}_2}{m},$$

$$\zeta_1 = \frac{\hat{\zeta}_1\beta_1}{\beta_2 m}, \zeta_2 = \frac{\hat{\zeta}_2}{m}, \sigma_1 = \frac{\hat{\sigma}_1}{m}, \sigma_2 = \frac{\hat{\sigma}_2}{m}, \sigma_3 = \frac{\hat{\sigma}_3}{m}, b_j = \frac{\eta\hat{b}_j}{m}, \text{ where } j = 1,2.$$

$$a_i = \frac{\hat{a}_i}{\hat{a}_1}, \text{ where } i = 2,3,4,5,6,7.$$

Then the system (3) are as follows:

$$\frac{dw}{dt} = T\left(1 - \frac{w}{w+1}\right)x - \frac{\delta_1 xw}{w+a_2} - \frac{\delta_2 yw}{w+a_3} - \frac{\delta_3 zw}{w+a_4} - w,$$

$$\frac{dx}{dt} = \left(\frac{Gw}{w+a_5} - x\right)x - \frac{xy}{x+b_1} - \frac{xz}{x+b_2} - \sigma_1 x,$$
$$\frac{dy}{dt} = \left(\frac{\nu_1 w^2}{w^2+a_6^2}\right)\left(\frac{xy}{x+b_1}\right) - \frac{\zeta_1 yz}{y+c} - \sigma_2 y,$$
$$\frac{dz}{dt} = \left(\frac{\nu_2 w^2}{w^2+a_7^2}\right)\left(\frac{xz}{x+b_2}\right) + \frac{\zeta_2 yz}{y+c} - \sigma_3 z. \tag{4}$$

As the primes and hats are removed for clarity, we focus on the parameters first. We obtain the most basic classical model (4). To maintain the dimension in the system (4) while fractionalizing the ordinary derivative, we introduce a new parameter $\eta^{\alpha-1}$ so that

$$\frac{d}{dt} \to \eta^{\alpha-1}\, {}_{t_0}^{C}D_t^{\alpha}, \tag{5}$$

where η exhibits a characteristic unit of time. Now, we establish the system (4) in the sense of Caputo FD.

$${}_{t_0}^{C}D_t^{\alpha} w(t) = \eta^{1-\alpha}\left(T\left(1 - \frac{w}{w+1}\right)x - \frac{\delta_1 wx}{w+a_2} - \frac{\delta_2 wy}{w+a_3} - \frac{\delta_3 wz}{w+a_4} - w\right),$$
$${}_{t_0}^{C}D_t^{\alpha} x(t) = \eta^{1-\alpha}\left(\left(\frac{Gw}{w+a_5} - x\right)x - \frac{xy}{x+b_1} - \frac{xz}{x+b_2} - \sigma_1 x\right),$$
$${}_{t_0}^{C}D_t^{\alpha} y(t) = \eta^{1-\alpha}\left(\left(\frac{\nu_1 w^2}{w^2+a_6^2}\right)\left(\frac{xy}{x+b_1}\right) - \frac{\zeta_1 yz}{y+c} - \sigma_2 y\right),$$
$${}_{t_0}^{C}D_t^{\alpha} z(t) = \eta^{1-\alpha}\left(\left(\frac{\nu_2 w^2}{w^2+a_7^2}\right)\left(\frac{xz}{x+b_2}\right) + \frac{\zeta_2 yz}{y+c} - \sigma_3 z\right), \tag{6}$$

with non-zero positive initial conditions $w(t_0)$, $x(t_0)$, $y(t_0)$, $z(t_0)$. Plankton and fish populations, and oxygen concentrations in aquatic ecosystems often exhibit complex dynamics. They can display irregular oscillations, transient behaviors, or even chaotic patterns. FDs can capture the intricate temporal dynamics of these systems, especially when the behavior is characterized by power-law relationships, non-exponential decay, or persistent memory effects. The FD allows for a more flexible and nuanced description of the growth and interactions between plankton, fish, and oxygen. Also, it has been shown that the FD is more successful in simulating real-world problems involving memory effects. In this context, memory refers to a sort of memory in which the dynamics of the present are influenced by the past. This sets off the defense mechanisms of some living organisms. In the context of the present model, the dynamics of the species and oxygen concentration in the water are the phenomena influenced by the memory we stated here.

4. Bondedness, Existence and uniqueness of the solution

In this section, we have established the boundedness, existence and uniqueness of the solution to the fractional marine system presented in equation (6).

Theorem 4.1. [20] Consider $\mho = \{(w, x, y, z) \in \mathbb{R}^4 : \|w\| < K_1, \|x\| < K_2, \|y\| < K_3, \|z\| < K_4\}$. All the solution of the system (6) starting in $\mho_+$ are bounded.

Proof. Let's start by defining a function $\psi(t) = w(t) + x(t) + y(t) + z(t)$. Using the Caputo type fractional derivative, we get

$$
\begin{aligned}
{}_{t_0}^{C}D_t^{\alpha}\psi(t)+\sigma_3\psi(t) &= {}_{t_0}^{C}D_t^{\alpha}[w(t)+x(t)+y(t)+z(t)]+\sigma_3(w(t)+x(t)+y(t)+z(t))\\
&= T\left(1-\frac{w}{w+1}\right)x-\frac{\delta_1 wx}{w+a_2}-\frac{\delta_2 wy}{w+a_3}-\frac{\delta_3 wz}{w+a_4}-w+\left(\frac{Gw}{w+a_5}-x\right)x\\
&\quad -\frac{xy}{x+b_2}-\sigma_1 x+\left(\frac{\nu_1 w^2}{w^2+a_6^2}\right)\left(\frac{xy}{x+b_1}\right)-\frac{\zeta_1 yz}{y+c}-\sigma_2 y+\left(\frac{\nu_2 w^2}{w^2+a_7^2}\right)\left(\frac{xz}{x+b_2}\right)\\
&\quad +\frac{\zeta_2 yz}{y+c}-\sigma_3 z+\sigma_3(w+x+y+z)\\
&\le Tx+\frac{Gwx}{w+a_5}+\left(\frac{\nu_1 w^2}{w^2+a_6^2}\right)\left(\frac{xy}{x+b_1}\right)+\left(\frac{\nu_2 w^2}{w^2+a_7^2}\right)\left(\frac{xz}{x+b_2}\right)+\frac{\zeta_2 yz}{y+c}+\sigma_3(w+x+y)\\
&= Tx+\frac{Gx}{1+\frac{a_5}{w}}+\left(\frac{\nu_1}{1+(\frac{a_6}{w})^2}\right)\left(\frac{y}{1+\frac{b_1}{x}}\right)+\left(\frac{\nu_2}{1+(\frac{a_7}{w})^2}\right)\left(\frac{z}{1+\frac{b_2}{x}}\right)+\frac{\zeta_2 z}{1+\frac{c}{y}}\\
&\quad +\sigma_3(w+x+y)\\
&\le Tx+Gx+\nu_1 y+\nu_2 z+\zeta_2 z+\sigma_3(w+x+y).
\end{aligned}
$$

The inequality described above may be simplified as:

$$
{}_{t_0}^{C}D_t^{\alpha}\psi(t)\le \sigma_3 K_1+(T+G+\sigma_3)K_2+(\nu_1+\sigma_3)K_3+(\nu_2+\zeta_2)K_4.
$$

Suppose, $\chi = max\{K_2, K_3, K_4\}$. Since, W represents oxygen concentration, we can not combined it with other compartment. Then,

$$
{}_{t_0}^{C}D_t^{\alpha}\psi(t)\le \sigma_3 K_1+(T+G+\nu_1+\nu_2+\zeta_2+2\sigma_3)\chi.
$$

By lemma2, we get

$$
\begin{aligned}
&{}_{t_0}^{C}D_t^{\alpha}\psi(t)+\sigma_3\psi(t)\le \left(\psi(t_0)-\frac{1}{\sigma_3}(\sigma_3K_1+(T+G+\nu_1+\nu_2+\zeta_2+2\sigma_3)\chi\right)E_\alpha[-\sigma_3(t-t_0)^\alpha]\\
&+\frac{1}{\sigma_3}(\sigma_3K_1+(T+G+\nu_1+\nu_2+\zeta_2+2\sigma_3)\chi).\\
&\to\frac{1}{\sigma_3}(\sigma_3K_1+(T+G+\nu_1+\nu_2+\zeta_2+2\sigma_3)\chi),\, t\to\infty.
\end{aligned}
$$

As a result, all of the solutions of the system (6) that begin in $\mho_+$ remain bounded in

$$
\theta = \{(w, x, y, z)\in \mho_+ | \psi(t)\le(\sigma_3K_1+(T+G+\nu_1+\nu_2+\zeta_2+2\sigma_3)\chi)+\varepsilon,\ \varepsilon>0\}.
$$

Theorem 4.2. Consider $\mho = \{(w, x, y, z)\in\mathbb{R}^4 : \|w\|<K_1, \|x\|<K_2, \|y\|<K_3, \|z\|<K_4\}$ and $\bar{\tau} < +\infty$. In the region $\mho\times[0,\bar{\tau}]$, the solution of the system (6) exists and is unique.

Proof. We consider $P(t) = (w(t), x(t), y(t), z(t))$, $\bar{P}(t) = (\bar{w}(t), \bar{x}(t), \bar{y}(t), \bar{z}(t))$ and a function as

$$
h(t, P) = (h_1(t, P), h_2(t, P), h_3(t, P), h_4(t, P)),
$$

where $h(t, P)$ is defined on $[0, \bar{\tau}] \times \mho$. Here,

$$h_1(t,P) = kT\left(1-\frac{w}{w+1}\right)x - \frac{k\delta_1 wx}{w+a_2} - \frac{k\delta_2 wy}{w+a_3} - \frac{k\delta_3 wz}{w+a_4} - kw,$$
$$h_2(t,P) = k\left(\frac{Gw}{w+a_5} - x\right)x - \frac{kxy}{x+b_1} - \frac{kxz}{x+b_2} - k\sigma_1 x,$$
$$h_3(t,P) = \left(\frac{k\nu_1 w^2}{w^2+a_6^2}\right)\left(\frac{xy}{x+b_1}\right) - \frac{k\zeta_1 yz}{y+c} - k\sigma_2 y,$$
$$h_4(t,P) = \left(\frac{k\nu_2 w^2}{w^2+a_7^2}\right)\left(\frac{xz}{x+b_2}\right) + \frac{k\zeta_2 yz}{y+c} - k\sigma_3 z. \tag{7}$$

where, $k = \eta^{1-\alpha}$. We inspect the norm as $\|P(t)\| = \sup_{t\in[0,\bar{\tau}]} |P(t)|$. Let $l = \sup_{\mho}\|h(t, P)\|$.

We shall prove that there exists some ξ, which implies that

$$\|h(P) - h(\bar{P})\| \le \xi\|P - \bar{P}\|. \tag{8}$$

Consider,

$$\begin{aligned}
\left\|h(P)-h(\bar{P})\right\| &= \left\|h_1(P)-h_1(\bar{P})\right\| + \left\|h_2(P)-h_2(\bar{P})\right\| + \left\|h_3(P)-h_3(\bar{P})\right\| + \left\|h_4(P)-h_4(\bar{P})\right\| \\
&= \left\|\frac{kTx}{w+1} - \frac{k\delta_1 wx}{w+a_2} - \frac{k\delta_2 wy}{w+a_3} - \frac{k\delta_3 wz}{w+a_4} - kw - \frac{kT\bar{x}}{\bar{w}+1} + \frac{k\delta_1 \bar{w}\bar{x}}{\bar{w}+a_2} + \frac{k\delta_2 \bar{w}\bar{y}}{\bar{w}+a_3} + \frac{k\delta_3 \bar{w}\bar{z}}{\bar{w}+a_4} + k\bar{w}\right\| \\
&+ \left\|\frac{kGwx}{w+a_5} - kx^2 - \frac{kxy}{x+b_1} - \frac{kxz}{x+b_2} - k\sigma_1 x - \frac{kG\bar{x}\bar{w}}{\bar{w}+a_5} + k\bar{x}^2 + \frac{k\bar{x}\bar{y}}{\bar{x}+b_1} + \frac{k\bar{x}\bar{z}}{\bar{x}+b_2} + k\sigma_1\bar{x}\right\| \\
&+ \left\|\left(\frac{k\nu_1 w^2}{w^2+a_6^2}\right)\left(\frac{xy}{x+b_1}\right) - \frac{k\zeta_1 yz}{y+c} - k\sigma_2 y - \left(\frac{k\nu_1 \bar{w}^2}{\bar{w}^2+a_6^2}\right)\left(\frac{\bar{x}\bar{y}}{\bar{x}+b_1}\right) + \frac{k\zeta_1 \bar{y}\bar{z}}{\bar{y}+c} + k\sigma_2\bar{y}\right\| \\
&+ \left\|\left(\frac{k\nu_2 w^2}{w^2+a_7^2}\right)\left(\frac{xz}{x+b_2}\right) + \frac{k\zeta_2 yz}{y+c} - k\sigma_3 z - \left(\frac{k\nu_2 \bar{w}^2}{\bar{w}^2+a_7^2}\right)\left(\frac{\bar{x}\bar{z}}{\bar{x}+b_2}\right) - \frac{k\zeta_2 \bar{y}\bar{z}}{\bar{y}+c} + k\sigma_3\bar{z}\right\| \\
&= \left\|-k(w-\bar{w}) + kT\left(\frac{(x-\bar{x})}{w+1} + \frac{\bar{x}(w-\bar{w})}{(w+1)(\bar{w}+1)}\right) - k\delta_1\left(\frac{w(x-\bar{x})}{w+a_2} + \frac{a_2\bar{x}(w-\bar{w})}{(w+a_2)(\bar{w}+a_2)}\right)\right. \\
&\quad \left. -k\delta_2\left(\frac{w(y-\bar{y})}{w+a_3} + \frac{a_3\bar{y}(w-\bar{w})}{(w+a_3)(\bar{w}+a_3)}\right) - k\delta_3\left(\frac{w(z-\bar{z})}{w+a_4} + \frac{a_4\bar{z}(w-\bar{w})}{(w+a_4)(\bar{w}+a_4)}\right)\right\| \\
&+ \left\|-k\sigma_1(x-\bar{x}) + kG\left(\frac{w(x-\bar{x})}{w+a_5} + \frac{a_5\bar{x}(w-\bar{w})}{(w+a_5)(\bar{w}+a_5)}\right) - k(x^2-\bar{x}^2)\right. \\
&\quad \left. -k\left(\frac{x(y-\bar{y})}{x+b_1} + \frac{b_1\bar{y}(x-\bar{x})}{(x+b_1)(\bar{x}+b_1)}\right) - k\left(\frac{x(z-\bar{z})}{x+b_2} + \frac{b_2\bar{z}(x-\bar{x})}{(x+b_2)(\bar{x}+b_2)}\right)\right\| \\
&+ \left\|-k\sigma_2(y-\bar{y}) + k\nu_1\left(\frac{w^2x(y-\bar{y})}{(w^2+a_6^2)(x+b_1)} + \frac{w^2\bar{y}b_1(x-\bar{x})}{(w^2+a_6^2)(x+b_1)(\bar{x}+b_1)}\right.\right. \\
&\quad \left.\left. + \frac{\bar{x}\bar{y}a_6^2(w^2-\bar{w}^2)}{(w^2+a_6^2)(\bar{w}^2+a_6^2)(\bar{x}+b_1)}\right) - k\zeta_1\left(\frac{y(z-\bar{z})}{y+c} + \frac{c\bar{z}(y-\bar{y})}{(y+c)(\bar{y}+c)}\right)\right\|
\end{aligned}$$

$$+\left\|-k\sigma_3(z-\bar{z})+k\nu_2\left(\frac{w^2x(z-\bar{z})}{(w^2+a_7^2)(x+b_2)}+\frac{w^2\bar{z}b_2(x-\bar{x})}{(w^2+a_7^2)(x+b_2)(\bar{x}+b_2)}\right.\right.$$
$$\left.\left.+\frac{\bar{x}\bar{z}a_7^2(w^2-\bar{w}^2)}{(w^2+a_7^2)(\bar{w}^2+a_7^2)(\bar{x}+b_2)}\right)+k\zeta_2\left(\frac{y(z-\bar{z})}{y+c}+\frac{c\bar{z}(y-\bar{y})}{(y+c)(\bar{y}+c)}\right)\right\|$$
$$\leq\|w-\bar{w}\|\left(k+kTK_2+\frac{k\delta_1K_2}{a_2}+\frac{k\delta_2K_3}{a_3}+\frac{k\delta_3K_4}{a_4}+\frac{kGK_2}{a_5}+\frac{2kK_1K_2K_3\nu_1}{a_6^2b_1}\right.$$
$$\left.+\frac{2k\nu_2K_1K_2K_4}{a_7^2b_2}\right)+\|x-\bar{x}\|\left(k(\sigma_1+T+2K_2)+\frac{k\delta_1K_1}{a_2}+\frac{kGK_1}{a_5}+\frac{kK_3}{b_1}+\frac{kK_4}{b_2}\right.$$
$$\left.+\frac{k\nu_1K_1^2K_3}{a_6^2b_1}+\frac{k\nu_2K_1^2K_4}{a_7^2b_2}\right)+\|y-\bar{y}\|\left(k\sigma_2+\frac{k\delta_2K_1}{a_3}+\frac{kK_2}{b_1}+\frac{k\nu_1K_1^2K_2}{a_6^2b_1}+\frac{kK_4}{c}(\zeta_1+\zeta_2)\right)$$
$$+\|z-\bar{z}\|\left(k\sigma_3+\frac{k\delta_3K_1}{a_4}+\frac{kK_1}{b_2}+\frac{k\nu_2K_1^2K_2}{a_7^2b_2}+\frac{kK_3}{c}(\zeta_1+\zeta_2)\right).$$

This implies

$$\|h(P)-h(\bar{P})\|\leq\xi_1\|w-\bar{w}\|+\xi_2\|x-\bar{x}\|+\xi_3\|y-\bar{y}\|+\xi_4\|z-\bar{z}\|,$$

where,

$$\xi_1=\left(k+kTK_2+\frac{k\delta_1K_2}{a_2}+\frac{k\delta_2K_3}{a_3}+\frac{k\delta_3K_4}{a_4}+\frac{kGK_2}{a_5}+\frac{2kK_1K_2K_3\nu_1}{a_6^2b_1}+\frac{2k\nu_2K_1K_2K_4}{a_7^2b_2}\right),$$
$$\xi_2=\left(k(\sigma_1+T+2K_2)+\frac{k\delta_1K_1}{a_2}+\frac{kGK_1}{a_5}+\frac{kK_3}{b_1}+\frac{kK_4}{b_2}+\frac{k\nu_1K_1^2K_3}{a_6^2b_1}+\frac{k\nu_2K_1^2K_4}{a_7^2b_2}\right),$$
$$\xi_3=\left(k\sigma_2+\frac{k\delta_2K_1}{a_3}+\frac{kK_2}{b_1}+\frac{k\nu_1K_1^2K_2}{a_6^2b_1}+\frac{kK_4}{c}(\zeta_1+\zeta_2)\right),$$
$$\xi_4=\left(k\sigma_3+\frac{k\delta_3K_1}{a_4}+\frac{kK_1}{b_2}+\frac{k\nu_2K_1^2K_2}{a_7^2b_2}+\frac{kK_3}{c}(\zeta_1+\zeta_2)\right). \tag{9}$$

where $\xi=\max\{\xi_1, \xi_2, \xi_3, \xi_4\}$. This gives as

$$\|h(P)-h(\bar{P})\|\leq\xi\,\|P-\bar{P}\|.$$

We will create a Picard's operator denoted by Δ which will be constructed by employing both the function h and fractional integral and this yields

$$\Delta P=P(0)+I^{\alpha}\,h(t,P). \tag{10}$$

We need to demonstrate that operator Δ is contraction mapping. Let

$$\|P-P(0)\|\leq\phi.$$

φ is a constant. Taking norm on (10), we obtain

$$\|\Delta P-P(0)\|\leq\|h(t,P)\|\,I^{\alpha}(1)$$
$$\leq l\frac{\bar{\tau}^{\alpha}}{\Gamma(\alpha+1)}<\phi. \tag{11}$$

If $\frac{\bar{\tau}^{\alpha}}{\Gamma(\alpha+1)} < \frac{\phi}{l}$, then the inequality (11) holds. We now arrive at a circumstance where the operator Δ is a contraction. The steps are as follows in order to fulfill this criterion.

$$\begin{aligned}\left\|\Delta P - \Delta \bar{P}\right\| &= \left\| I^{\alpha}(h(t,P) - h(t,\bar{P}))\right\| \\ &\leq I^{\alpha}\left\|h(t,P) - h(t,\bar{P})\right\| \\ &\leq \left\|h(t,P) - h(t,\bar{P})\right\| I^{\alpha}(1) \\ &\leq \frac{\bar{\tau}^{\alpha}}{\Gamma(\alpha+1)}\xi\left\|P - \bar{P}\right\|. \end{aligned} \tag{12}$$

Equation (12) represents that when

$$\frac{\bar{\tau}^{\alpha}}{\Gamma(\alpha+1)} \leq \frac{1}{\xi},$$

the Picard's operator Δ behave as contraction. This proves the contraction of the Picard's operator Δ. Using the Banach fixed point theorem, we can conclude that the operator Δ has a unique fixed point. Consequently, the fractional differential equation given in equation (6) has a unique solution, but only when $\frac{\bar{\tau}^{\alpha}}{\Gamma(\alpha+1)}$ is less than the minimum value between $\frac{\phi}{l}$ and $\frac{1}{\xi}$

5. Equilibrium points

To evaluate the points of equilibria of the system (6), we set

$${}_{t_0}^{C}D_t^{\alpha} w = 0,\ {}_{t_0}^{C}D_t^{\alpha} x = 0,\ {}_{t_0}^{C}D_t^{\alpha} y = 0,\ {}_{t_0}^{C}D_t^{\alpha} z = 0.$$

By observation, the system (6) has five equilibrium points.

1. For any set of parameter values, the trivial equilibrium point $A_0 = (0, 0, 0, 0)$ always exists.
2. The predators free equilibrium point is $A_1 = (w_1, x_1, 0, 0)$. In this case, the main autotroph in the system, phytoplankton, generates oxygen since there are no zooplankton or fish present in the population. With the annihilation of zooplankton and fish the system (6) reduce to the oxygen-phytoplankton sub-system (13) and (14).

$${}_{t_0}^{C}D_t^{\alpha} w(t) = kT\left(1 - \frac{w}{w+1}\right)x - \frac{k\delta_1 w x}{w + a_2} - kw. \tag{13}$$

$${}_{t_0}^{C}D_t^{\alpha} x(t) = k\left(\frac{Gw}{w + a_5} - x\right)x - k\sigma_1 x. \tag{14}$$

Therefore, the oxygen and phytoplankton isoclines are shown by:

$$x_1 = \frac{w_1(w_1+1)(w_1+a_2)}{Ta_2 + (T-\delta_1)w_1 - \delta_1 w_1^2},\ x_1 = \frac{Gw_1}{w_1 + a_5} - \sigma_1. \tag{15}$$

3. The fish free equilibrium point is $A_2 = (w_2, x_2, y_2, 0)$.

In the absence of fish population, the oxygen, phytoplankton, and zooplankton isocline are given by:

$$w_2 = \frac{a_5(x_2 + \frac{y_2}{x_2 + b_1} + \sigma_1)}{G - \frac{y_2}{x_2 + b_1} - x_2 - \sigma_1},\ x_2 = \frac{\sigma_2 b_1 (w_2^2 + a_6^2)}{\nu_1 w_2^2 - \sigma_2 (w_2^2 + a_6^2)},$$
$$y_2 = \frac{w_2 + a_3}{\delta_2}\left(\frac{Tx_2}{w_2(w_2+1)} - \frac{\delta_1 x_2}{w_2 + a_2} - 1\right). \tag{16}$$

4. The zooplankton free equilibrium point is $A_3 = (w_3, x_3, 0, z_3)$.
   In the absence of the zooplankton population, then the oxygen, phytoplankton, and fish isocline are given by:

$$w_3 = \frac{a_5(x_3 + \frac{z_3}{x_3 + b_2} + \sigma_1)}{G - \sigma_1 - x_3 - \frac{z_3}{x_3 + b_2}},\ x_3 = \frac{\sigma_3 b_2 (w_3^2 + a_7^2)}{\nu_2 w_3^2 - \sigma_3 (w_3^2 + a_7^2)},$$
$$z_3 = \frac{w_3 + a_4}{\delta_3}\left(\frac{Tx_3}{w_3(w_3+1)} - \frac{\delta_1 x_3}{w_3 + a_2} - 1\right). \tag{17}$$

5. The coexistence equilibrium point is $A_4 = (w_4, x_4, y_4, z_4)$.
   The coexistence equilibrium A_4 reaches a stable state when:

$$w_4 = \frac{a_5\left(x_4 + \frac{y_4}{x_4 + b_1} + \frac{z_4}{x_4 + b_2} + \sigma_2\right)}{G - x_4 - \frac{y_4}{x_4 + b_1} - \frac{z_4}{x_4 + b_2} - \sigma_2},\ x_4 = \frac{b_2(\frac{\zeta_2 y_4}{y_4 + c} + \sigma_3)}{\frac{\nu_2 w_4^2}{w_4^2 + a_4^2} - \frac{\zeta_2 y_4}{y_4 + c} - \sigma_3},$$
$$y_4 = \frac{w_4 + a_3}{\delta_2}\left(\frac{Tx_4}{w_4(w_4+1)} - \frac{\delta_1 x_4}{w_4 + a_2} - \frac{\delta_3 z_4}{w_4 + a_3} - 1\right),$$
$$z_4 = \frac{y_4 + c}{\zeta_1}\left(\left(\frac{\nu_1 w_4^2}{w_4^2 + a_6^2}\right)\left(\frac{x_4}{x_4 + b_1}\right) - \sigma_2\right), \tag{18}$$

The Jacobian matrix of the system (6) is as follows:

$$J = \begin{pmatrix} l_{11} & l_{12} & l_{13} & l_{14} \\ l_{21} & l_{22} & l_{23} & l_{24} \\ l_{31} & l_{32} & l_{33} & l_{34} \\ l_{41} & l_{42} & l_{43} & l_{44}. \end{pmatrix} \tag{19}$$

$$l_{11} = -\frac{kTx}{(w+1)^2} - \frac{ka_2\delta_1 x}{(w+a_3)^2} - \frac{ka_3\delta_2 y}{(w+a_3)^2} - \frac{ka_4\delta_3 z}{(w+a_4)^2} - k,\ l_{12} = \frac{kT}{w+1} - \frac{kw\delta_1}{w+a_2},\ l_{13} = -\frac{k\delta_2 w}{w+a_3},\ l_{14} = -\frac{k\delta_3 w}{w+a_4},$$

$$l_{21} = \frac{kGxa_5}{(w+a_5)^2}, l_{22} = \frac{kGw}{w+a_5} - 2kx - \frac{kyb_1}{(x+b_1)^2} - \frac{kzb_2}{(x+b_2)^2} - k\sigma_1, l_{23} = -\frac{kx}{x+b_1}, l_{24} = -\frac{kx}{x+b_2},$$

$$l_{31} = \frac{2kv_1 a_6^2 wxy}{(w^2+a_6^2)(x+b_1)}, l_{32} = \frac{kw^2 yv_1 b_1}{(w^2+a_6^2)(x+b_1)^2}, l_{33} = \frac{kw^2 xv_1}{(w^2+a_6^2)(x+b_1)} - \frac{kz\zeta_1 c}{(y+c)^2} - k\sigma_2, l_{34} = -\frac{ky\zeta_1}{y+c},$$

$$l_{41} = \frac{2ka_7^2 v_2 wxz}{(w^2+a_7^2)^2(x+b_2)}, l_{42} = \frac{kv_2 b_2 w^2 z}{(w^2+a_7^2)(x+b_2)^2}, l_{43} = \frac{kcz\zeta_2}{(y+c)^2}, l_{44} = \frac{kv_2 w^2 x}{(w^2+a_7^2)(x+b_2)} + \frac{k\zeta_2 y}{y+c} - k\sigma_3.$$

The eigen values for every steady state A_0, A_1, A_2, A_3, and A_4 means the solutions of the subsequent characteristic equation:

$$det(J_i - \lambda I) = 0, \tag{20}$$

where the matrix J_i, $i = 1(1)4$ is given by (19) at the steady state A_0, A_1, A_2, A_3, and A_4 respectively and I is the unit matrix. Stability of the points of equilibrium can be seen by Theorem 2.1.

6. Numerical Simulation

In this part, we consider the generalized Predictor-Corrector numerical technique specified in [43, 44] for solving the fractional order system (6). We analyzed the dynamic response of the theoretical oxygen-plankton-fish system given in equation (6). To perform this analysis, we used hypothetical parameter values such as $G = 1.84$, $\delta_1 = 1$, $\delta_2 = 0.01$, $\delta_3 = 0.02$, $a_5 = 0.7$, $\sigma_1 = 0.07$, $\sigma_2 = 0.1$, $\sigma_3 = 0.1$, $b_1 = 0.1$, $b_2 = 1$, $v_1 = 0.7$, $v_2 = 0.9$, $\zeta_1 = 0.04$, $\zeta_2 = 0.6$, $c = 1$, and $a_i = 1$ for $i = 2, 3, 4, 5, 6, 7$. Then, we varied the values of α and T within a specific range to analyze the system's behavior. Initial conditions are considered as $w_0 = 0.385$, $x_0 = 0.3$, $y_0 = 0.1$, $z_0 = 0.12$. To ensure biological relevance, it is essential that all components and coefficients of the system are non-negative. Our main objective is to obtain an approximate solution of the oxygen-plankton-fish model (6) and analyze it using the Caputo-type fractional operator.

Figure 1 and 2 illustrate the solution profiles of system (6) for different fractional orders, namely $\alpha = 1$, $\alpha = 0.95$, $\alpha = 0.9$, and $\alpha = 0.85$ with a fixed amount of oxygen produced within the phytoplankton cells that is $T = 2.12$. Figure 1 depicts the effect of oxygen concentration on plankton and fish population, as well as the correlation between plankton and fish populations for different fractional orders. Figure 2 is the presentation of the dynamics of the four compartments with respect to time. For $\alpha = 1$, we have observed that all the compartments tends to extinction after some time particularly afer $t = 500$. This indeed a rare circumstances. For $\alpha = 0.85$ and $T = 2.12$, the system displays damped oscillations before converging towards an estimated steady state, which supports coexistence. On the other hand, for $\alpha = 0.9$ and $\alpha = 0.95$, the system exhibits periodic oscillations that expand over time.

Photosynthesis is one of the most fascinating processes on the planet. Temperature change is the most important factor that affects photosynthesis [45]. It was discussed in [7, 14] that the local water temperature influences on photosynthesis rate and therefore the production of oxygen varies day-to-day [46, 47]. Factor T, the oxygen generated within the phytoplankton cells, is a temperature-dependent parameter in the oxygen-plankton-fish system (6). To capture this dependence and to investigate the impact of temperature on the dynamics of the population, we have defined T as a linear function of time with global temperature as positive slope [7, 48].

$$T = T_0 \quad for\ t < t_0, \qquad T = T_0 + \omega\,(t - t_0)\ for\ t \geq t_0. \tag{21}$$

Here, t_0 is the initial time at which global warming commenced, T_0 is the rate of oxygen production before the change and ω is the rate of global warming.

Considering the temperature-dependent nature of the function T, we incorporate numerical simulations to determine this dependence. To observe the impact of $T(t)$ on system dynamics, we aim to

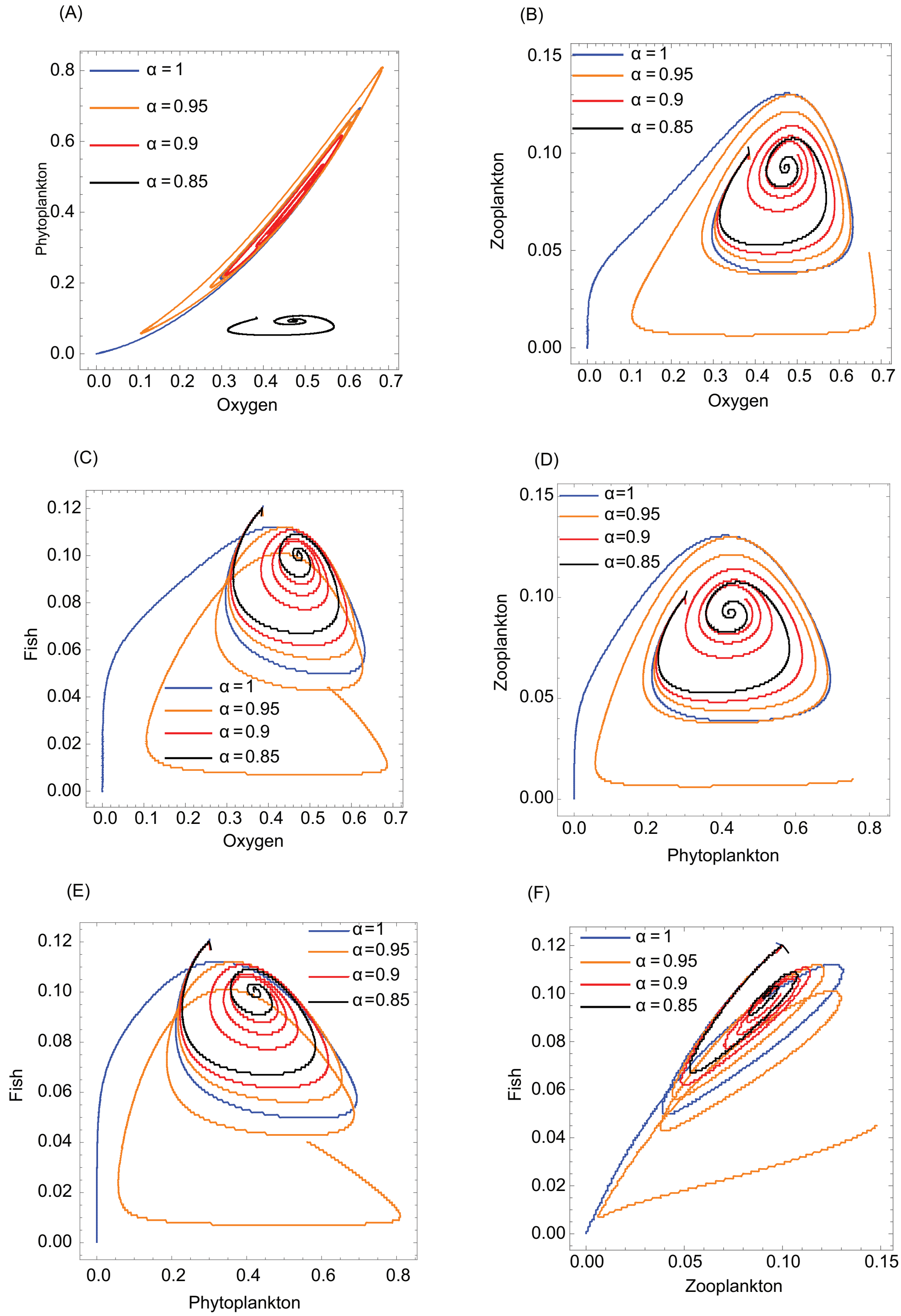

Figure 1: Two dimensional view of (A) phytoplankton versus oxygen, (B) zooplankton versus oxygen , (C) fish versus oxygen, (D) zooplankton versus phytoplankton, (E) fish versus phytoplankton, (F) fish versus zooplankton for different fractional orders at $T = 2.12$.

minimize the parameter representing global warming, denoted as ω. In Figures 2 to 7, we illustrate the system dynamics as the value of T and ω change over time. Specifically, the positive slopes in Figures 3(a), 5(a), 6(a), and 7(a) represent the variation of T with time. These visualizations provide a clearer understanding of the relationship between species population and changing oxygen concentrations.

Figure 3 depicts the changes in plankton and fish populations, as well as oxygen concentration, over time. The simulations were conducted for a initial rate of oxygen production $T_0 = 2$, with a warming rate of $\omega = 2 \times 10-5$, while considering different fractional orders. We observe that the density of phytoplankton and zooplankton is directly proportional to the oxygen concentration. However, the fish population exhibits an increase due to their physiological ability to adapt to low ppm levels of dissolved oxygen in water by enhancing the flow of water over their gills. This phenomenon was observed for decreasing values of the fractional order α. Figure 4 provides a two-dimensional (2D) visualization of the same dataset, presenting a graphical representation of the interrelationships among plankton and fish populations and oxygen concentration.

In Figure 5, we have considered the warming rate $\omega = 2 \times 10^{-5}$ and $T_0 = 2.011$. At $\alpha = 0.999$, because the oxygen concentration reaches the extinction state, plankton and fish density approach the point of extinction. The system exhibits periodic oscillation with a size reduction beforehand, and

subsequently, it develops the periodic oscillation with a raise in amplitude for different values of α. The amplitude of the oscillation is proportional to the warming. The system expands oscillations with larger amplitude, while the species population and oxygen concentration decrease. For $\alpha = 0.97$, in Figure 5, we observe that dynamics of oxygen concentration, phytoplankton, zooplankton and fish show indentical oscillation pattern upto $t = 3000$. If we observe the period between $t = 3000$ and $t =$

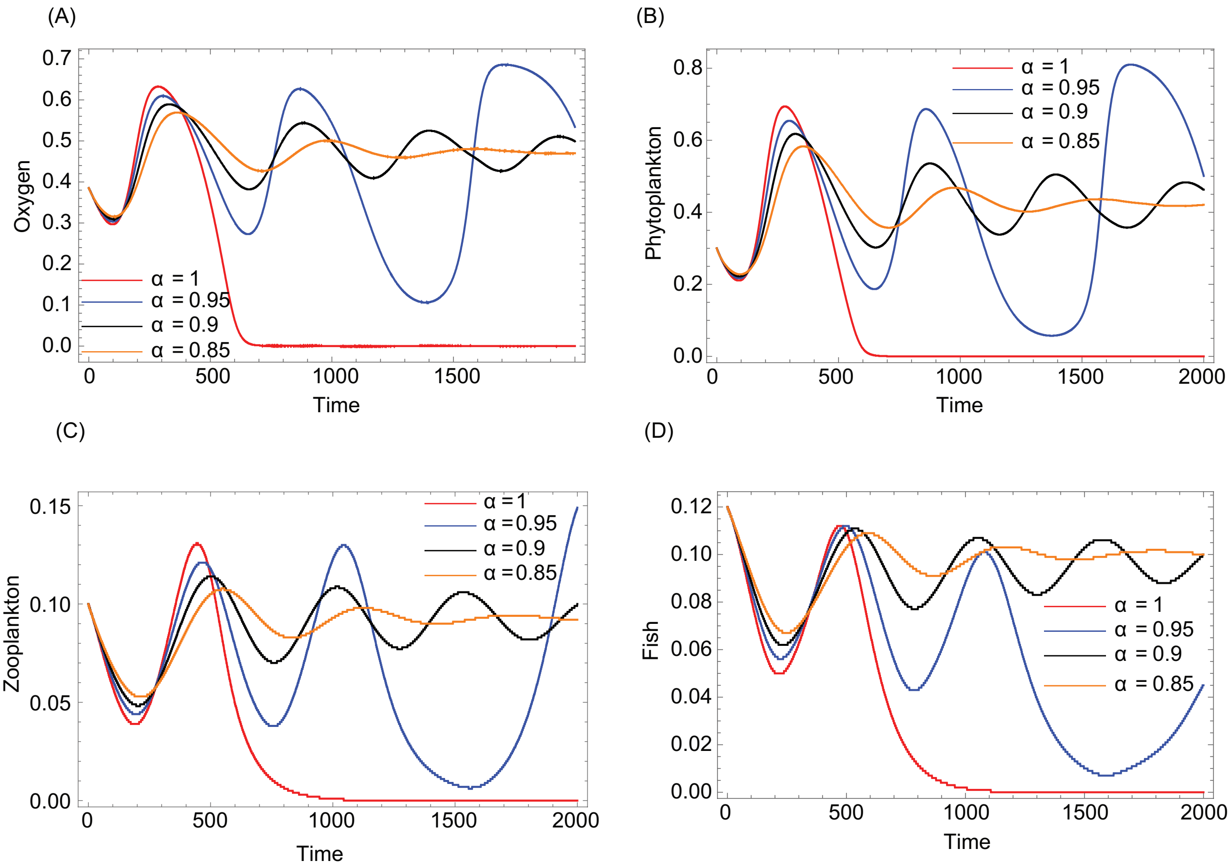

Figure 2: Fluctuation of (A) oxygen concentration, (B) phytoplankton density, (C) zooplankton density, (D) fish density with respect to time for $T = 2.12$.

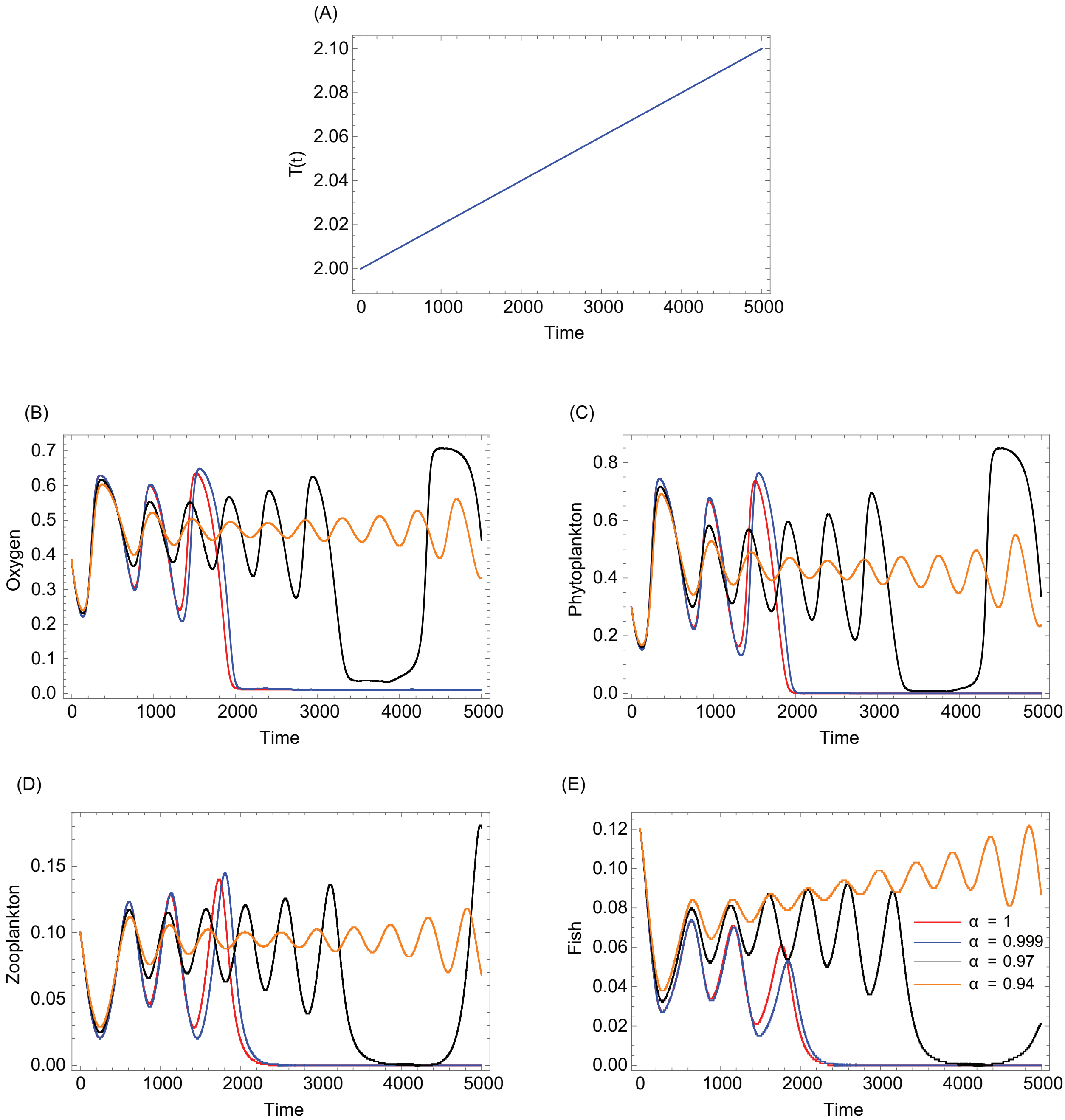

Figure 3: (A) Slope of temperature function versus time, (B) oxygen concentration, (C) phytoplankton density, (D) zooplankton density, (E) fish density versus time attained for $T_0 = 2$ and $\omega = 2 \times 10^{-5}$.

4000, even though oxygen, phyoplankton and zooplankton has the largest amplitude, fish population has the smallest amplitude. This means when all the other compartments are at their peak of growth, fishes are of at their lowest growth. This interesting phenomena, which can only be noticed under fractional order derivative, has high significance. We observe that at $t = 3000$ all the compartments experienced their fall. Microscopic organism plankton can grow faster once they get the environment. But the reproduction and recruitment of fishes are often influenced by factors such as maturity age, breeding cycle, and envirnmental condition. That means $\alpha = 0.97$ depicted a situation where fish population experinences a time lag in this response to the increased availability of oxygen and plankton.

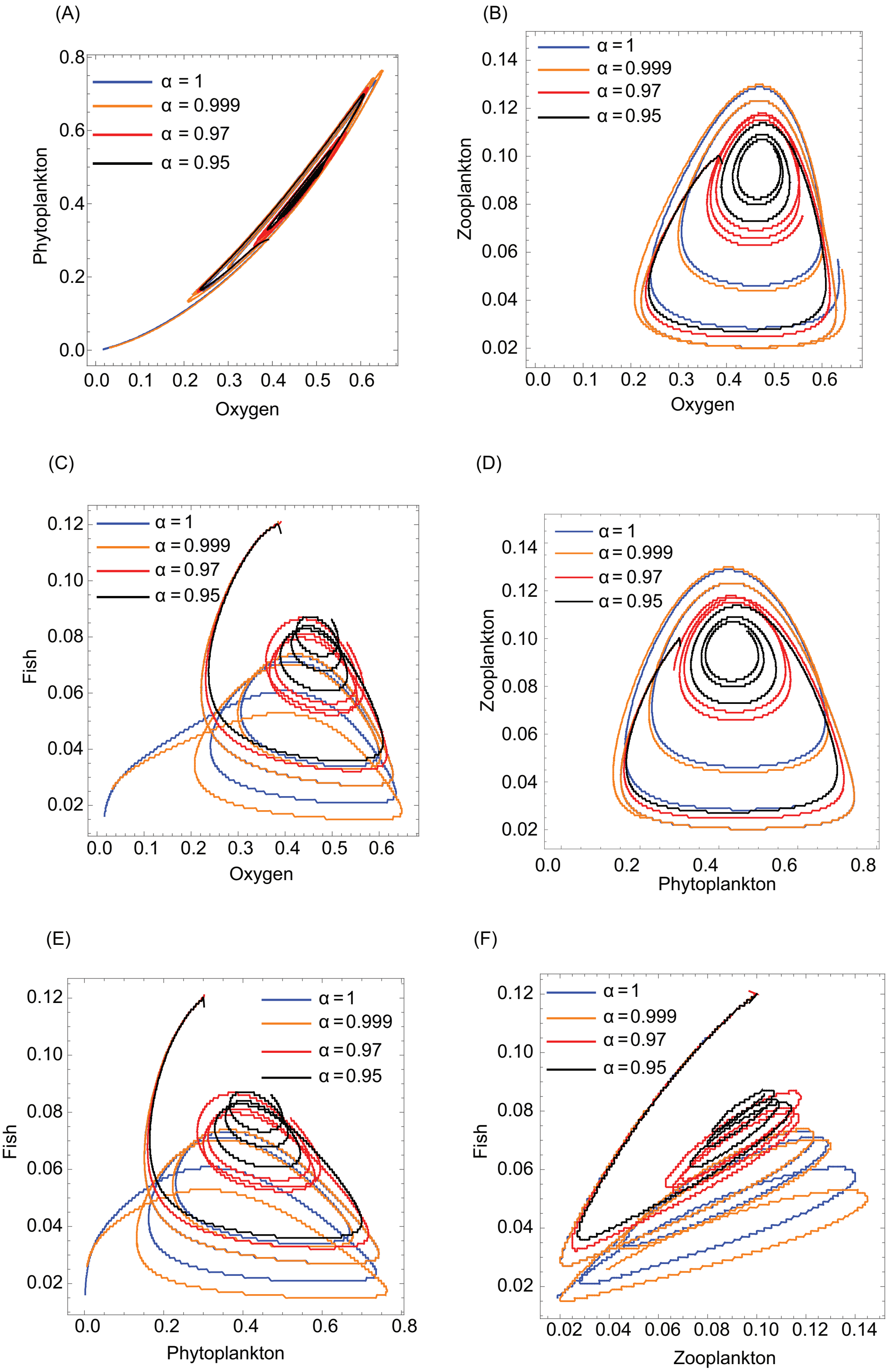

Figure 4: Two dimensional view of (A) phytoplankton versus oxygen, (B) zooplankton versus oxygen, (C) fish versus oxygen, (D) zooplankton versus phytoplankton, (E) fish versus phytoplankton, (F) fish versus zooplankton for $T_0 = 2$ and $\omega = 2 \times 10^{-5}$.

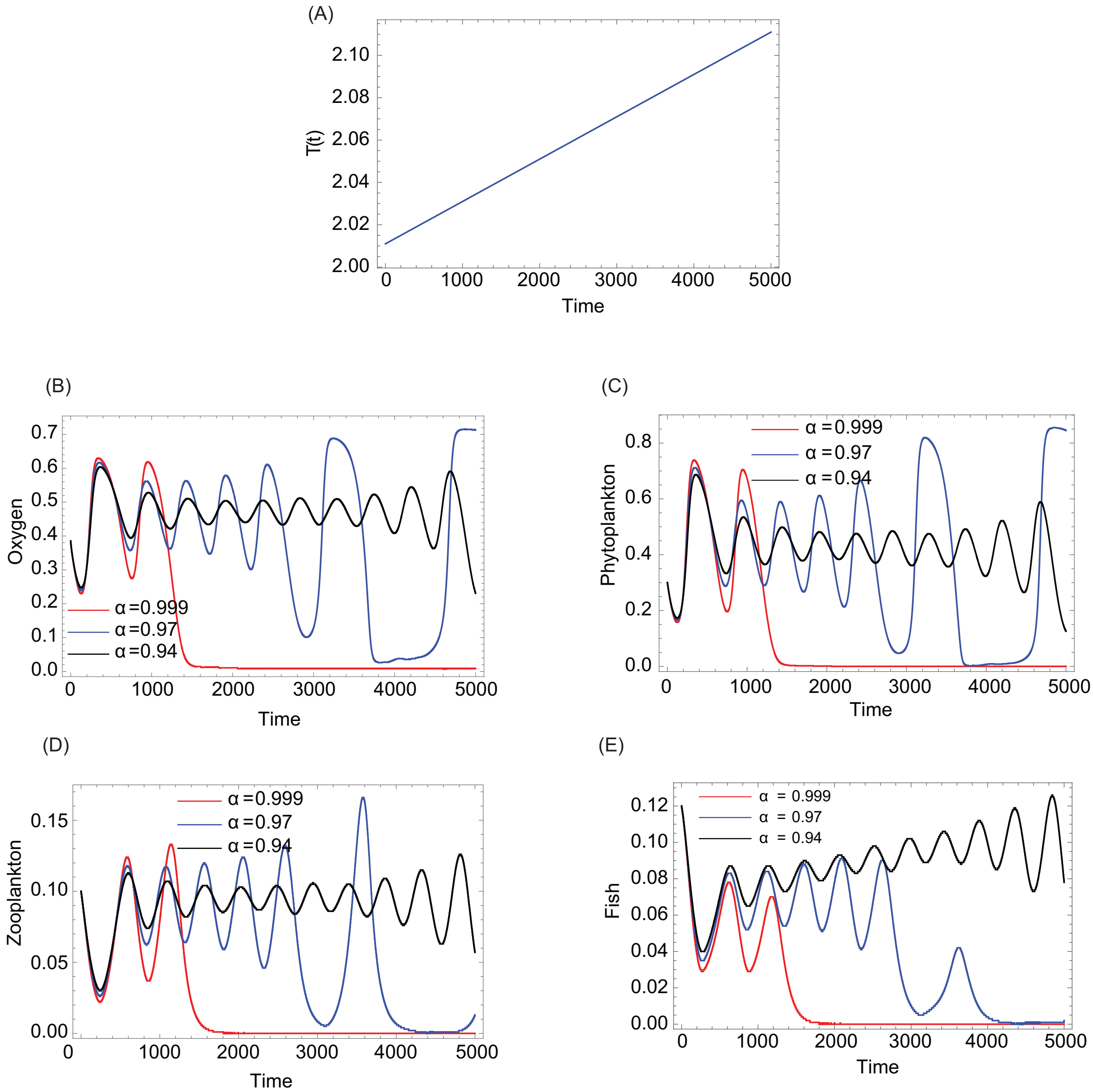

Figure 5: (A) Slope of temperature function versus time, (B) oxygen concentration, (C) phytoplankton density, (D) zooplankton density, (E) fish density versus time attained for $T_0 = 2.011$ and $\omega = 2 \times 10^{-5}$.

Now in Figure 6, we have increased the global warming rate to $\omega = 10^{-4}$ keeping initial oxygen concentration same as $T_0 = 2.011$. Here the extinction dynamics can be observed for $\alpha = 0.999$. Rise in global warming caused early extinction. But other fractional derivative values away from 1 demonstrate interesting observation. With this increased global warming rate, amplitude of oscillation increased in each compartment. This can be interpreated as a more relaiable observation because increase in global warming disturb all species on earth. In figure 7, we observe the impact of initial oxygen production by phytoplankton. Comparing the figures, we see that change in global warming impacts the amplitude of oscillation more than the change in oxygen concentration T_0. Influence of the fish population can be observed when we compare the results of the present work with these of [14]. In [14], for increasing value of α for $T_0 = 2.011$ and $\omega = 2 \times 10^{-5}$ the system exhibits periodic oscillation whereas present model exhibits non-periodic oscillation. Again for $T_0 = 2.065$ and $\omega = 10^{-4}$ all the values of α advocate extinction dynamics in [14]. whereas the present model exhibits co-existence

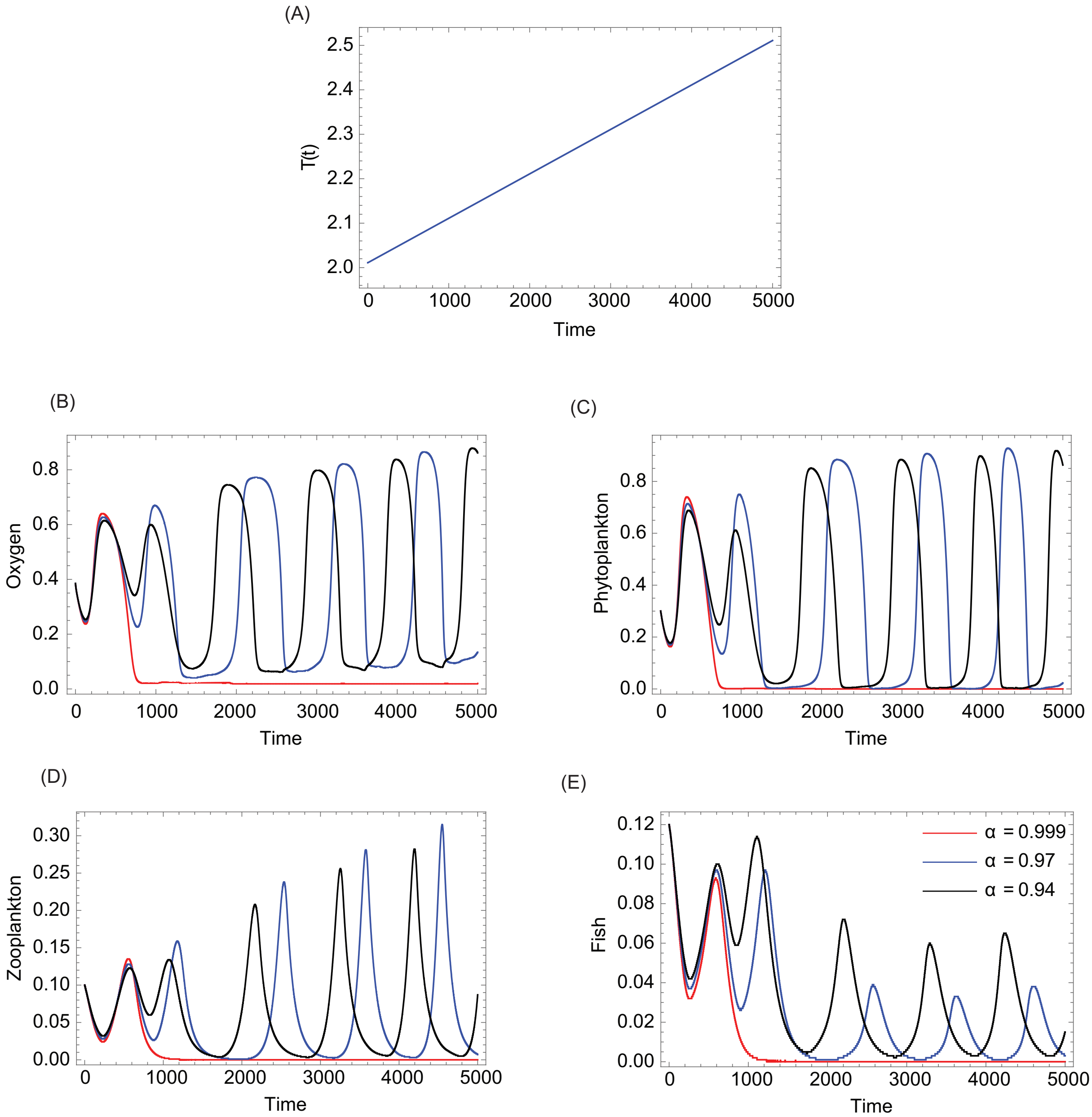

Figure 6: (A) Slope of temperature function versus time, (B) oxygen concentration, (C) phytoplankton density, (D) zooplankton density, (E) fish density versus time attained for distinct fractional order and for $T_0 = 2.011$ and $\omega = 10^{-4}$.

dynamics for α away from 1. Figure (3a), (5a), (6a), and (7a), reveal that oxygen prodecued in the cell of phytoplankton drops with the incease in the global warming. In the figures above, we have noticed that when α is very closed to 1, all the compartments namely oxygen, phytoplankton, zooplankton, and fishes go to extinction after certain period of time. But, that can not be a realistic representation of a ecologycal environment. Derivative values away from 1 display the circumstances of coexistence.

7. Conclusion

We utilized the Caputo fractional derivative to investigate the impact of global warming on the dynamics of oxygen concentration, plankton, and fish. Our study stands out for incorporating fish into the analysis of plankton dynamics, given their significance in the marine ecosystem as major oxygen consumers. We assumed that the rate of oxygen production is time-regulated and that temperature

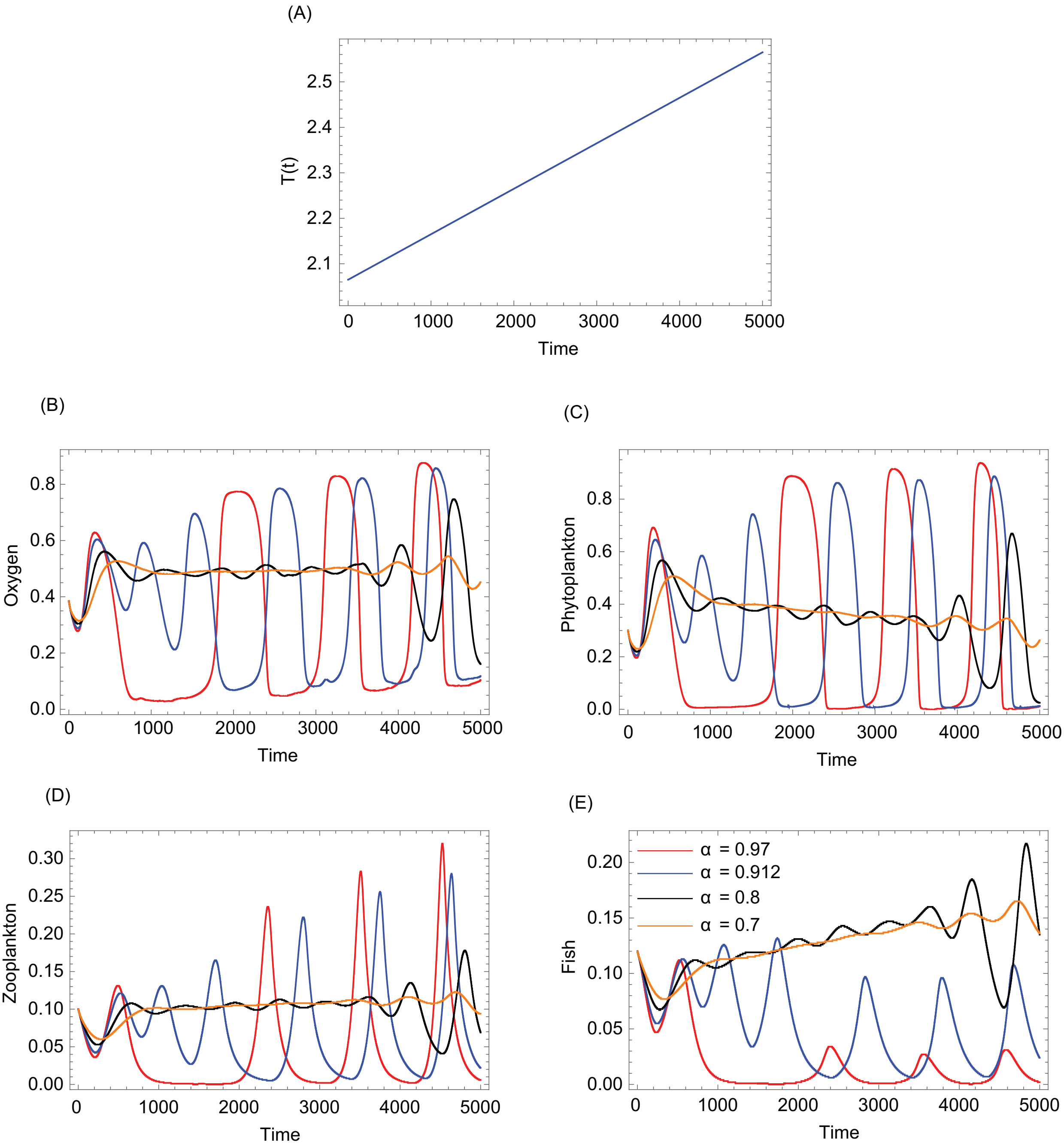

Figure 7: (A) Slope of temperature function versus time, (B) oxygen concentration, (C) phytoplankton density, (D) zooplankton density, (E) fish density versus time for $T_0 = 2.065$ and $\omega = 10^{-4}$.

increase is proportional to global warming. The theoretical properties of the proposed model were analyzed, including uniqueness, and existence of solution. We examined how different values of α affect oscillation type and size, finding that integer-order derivatives lead to extinction more quickly than FD. We also found that α can regulate system stability. We explored the effect of initial oxygen production (T_0) and global warming on dissolved oxygen, plankton, and fish population dynamics for various fractional values of α . It is noticed that higher initial oxygen production and global warming lead to extinction in interger order derivative sense and also for derivatives very close to one. But, a realistic representation of a ecologycal environment, which is survival dynamics, can be observed for derivative values away from 1. So, fractional derivative may be considered as the measures to be taken for sustainability of a certain ecological phenomena. Notably, the rate of oxygen production is inversely proportional to temperature in this scenario. Our study demonstrated that the Caputo fractional derivatives can help analyze the coexistence of elements and species in the marine ecosystem, suggesting further research into the impact of global warming on algae and coral dynamics.

Acknowledgment

Researchers would like to thank the Deanship of Scientific Research, Qassim University for funding publication of this project.

Conflict of interest

The authors declare no conflict of interest.

References

[1] J. H. Steele, *Spatial pattern in plankton communities*, vol. 3. Springer Science & Business Media, 1978.
[2] O. Akira, "Diffusion and ecological problems:(mathematical models)," *Biomathematics*, 1980.
[3] M. John P, "Ecological consequences of recent climate change," *Conserv Biol*, vol. 15, pp. 320–331, 2001.
[4] M. Horst, *Spatiotemporal patterns in ecology and epidemiology: theory, models, and simulation*. Chapman and Hall/CRC, 2007.
[5] H. Graham, *Phytoplankton ecology: structure, function and fluctuation*. Springer Science & Business Media, 2012.
[6] J. Lukas, H. Helmut, and K. Michal, "Global change drives modern plankton communities away from the pre-industrial state," *Nature*, vol. 570, pp. 372–375, 2019.
[7] Y. Sekerci and S. Petrovskii, "Mathematical modelling of plankton-oxygen dynamics under the climate change," *Bulletin of mathematical biology*, vol. 77, 2015.
[8] P. Yongzhen, L. Yunfei, and L. Changguo, "Evolutionary consequences of harvesting for a two-zooplankton one-phytoplankton system," *Applied Mathematical Modelling*, vol. 36, no. 4, pp. 1752–1765, 2012.
[9] M. Benfort, U. Feudel, M. Hilker, F, and H. Malchow, "Plankton blooms and patchiness generated by heterogeneous physical environment," *Ecol. Complexity*, no. 20, pp. 185 – 194, 2014.
[10] Lewis, N. D., Morozov, A., Breckels, M. N., Steinke, M., and Codling, E. A., "Multitrophic interactions in the sea: Assessing the effect of infochemical-mediated foraging in a 1-d spatial model," *Math. Model. Nat. Phenom.*, vol. 8, no. 6, pp. 25–44, 2013.
[11] S. V. Petrovskii and M. Horst, *Mathematical Models of Marine Ecosystem, Mathematical Models*, vol. 3. Eolss, 2009.
[12] T. Zhang and W. Wang, "Hopf bifurcation and bistability of a nutrient-phytoplankton-zooplankton model," *Applied Mathematical Modelling*, vol. 36, no. 12, pp. 6225–6235, 2012.
[13] A. K. Mishra, "Modeling the depletion of dissolved oxygen in a lake due to submerged macrophytes," *Nonlinear Analysis: Modelling and Control*, vol. 15, no. 2, pp. 185–198, 2010.
[14] R. Ozarsian and Y. Sekerci, "Fractional order oxygen-plankton system under climate change," *Chaos*, vol. 30, 2020.
[15] M. Caputo and M. Fabrizio, "A new definition of fractional derivatives without singular kernal," *Progr.Fract Differ Appl*, vol. 1, pp. 1–13, 2015.
[16] A. Atangana and D. Baleanu, "New fractional derivatives with non-local and non-singular kernel theory and application to heat transfer model," *Thermal Science*, vol. 20, pp. 763–769, 2016.
[17] A. Kumar, A. Prakash, and H. M. Baskonus, "The epidemic COVID-19 model via Caputo–Fabrizio fractional operator," *Waves in Random and Complex Media*, pp. 1–15, 05 2022.
[18] W. Gao and H. M. Baskonus, "Deeper investigation of modified epidemiological computer virus model containing the caputo operator," *Chaos, Solitons & Fractals*, vol. 158, 05 2022.
[19] S. J. Achar, C. Baishya, and M. K. Kaabar, "Dynamics of the worm transmission in wireless sensor network in the framework of fractional derivatives," *Mathematical Methods in the Applied Sciences*, 2021.
[20] C. Baishya, S. J. Achar, P. Veeresha, and D. G. Prakasha, "Dynamics of a fractional epidemiological model with disease infection in both the populations," *Chaos: An Interdisciplinary Journal of Nonlinear Science*, vol. 31, no. 4, 2021.
[21] Z. Hammouch, M. Yavuz, and N. Ozdemir, "Numerical solutions and synchronization of a variable-order fractional chaotic system," *Mathematical Modelling and Numerical Simulation with Applications*, vol. 1, pp. 11–23, 08 2021.
[22] C. Baishya and P. Veeresha, "Laguerre polynomial-based operational matrix of integration for solving fractional differential equations with non-singular kernel," *Proceedings of the Royal Society A*, vol. 477, 2021.
[23] C. Baishya, "An operational matrix based on the independence polynomial of a complete bipartite graph for the Caputo fractional derivative," *SeMA Journal*, pp. 1–19, 2021.

[24] R. S. Dubey, P. Goswami, H. M. Baskonus, and A. Tailor, "On the existence and uniqueness analysis of fractional blood glucose-insulin minimal model," *International Journal of Modeling, Simulation, and Scientific Computing*, 05 2022.

[25] M. Sajid, H. Chaudhary, A. Ali, and K. Santosh, "Chaos controllability in fractional-order systems via active dual combination–combination hybrid synchronization strategy," *Fractal and Fractional*, vol. 6, no. 11, 717, 2022.

[26] M. Yavuz, "European option pricing models described by fractional operators with classical and generalized Mittag-Leffler kernels," *Numerical Methods for Partial Differential Equations*, vol. 38, pp. 434–456, 05 2022.

[27] S. Djillali, A. Atangana, A. Zeb, and C. Park, "Mathematical analysis of a fractional-order epidemic model with nonlinear incidence function," *AIMS Mathematics*, vol. 7, no. 2, pp. 2160–2175, 2022.

[28] B. Dhar, P. K. Gupta, and M. Sajid, "Solution of a dynamical memory effect COVID-19 infection system with leaky vaccination efficacy by non-singular kernel fractional derivatives," *Mathematical Biosciences and Engineering*, vol. 19, no. 5, pp. 4341–4367, 2022.

[29] R. Singh, J. Mishra, and V. K. Gupta, "The dynamical analysis of a tumor growth model under the effect of fractal fractional Caputo-Fabrizio derivative," *International Journal of Mathematics and Computer in Engineering*, vol. 1, no. 1, 2023.

[30] B. Ghanbari and J. Gomez-Aguilar, "Modeling the dynamics of nutrient-phytoplankton-zooplankton system with variable-order fractional derivatives," *Chaos, Solitons & Fractals*, vol. 116, pp. 114–120, 2018.

[31] B. Ghanbari and S. Djilali, "Mathematical analysis of a fractional-order predator-prey model with prey social behavior and infection developed in predator population," *Chaos, Solitons & Fractals*, vol. 138, 2020.

[32] R. Shi, J. Ren, and C. Wang, "Stability analysis and hopf bifurcation of a fractional order mathematical model with time delay for nutrient-phytoplankton-zooplankton," *Mathematical Biosciences and Engineering*, vol. 17, no. 4, pp. 3836–3868, 2020.

[33] P. Veeresha and L. Akinyemi, "Fractional approach for mathematical model of phytoplankton-toxic phytoplankton-zooplankton system with mittag-leffler kernel," *International Journal of Biomathematics*, vol. 16, no. 03, 2023.

[34] M. Javidi and B. Ahmad, "Dynamic analysis of time fractional order phytoplankton-toxic phytoplankton-zooplankton system," *Ecological Modelling*, vol. 318, pp. 8–18, 2015. Ecological management for human-dominated urban and regional ecosystems.

[35] M. El-Shahed, A. Ahmed, and I. Elsony, "Fractional order model of phytoplankton-toxic phytoplankton-zooplankton system," *Advances in Analysis*, vol. 3, pp. 37–51, 01 2018.

[36] A. Yusuf, B. Acay, and M. Inc, "Analysis of fractional-order nonlinear dynamic systems under caputo differential operator," *Mathematical Methods in the Applied Sciences*, vol. 44, no. 13, pp. 10861–10880, 2021.

[37] S. Eze and M. Oyesanya, "Fractional order climate change model in a pacific ocean," *Journal of Fractional Calculus and Applications*, vol. 10, pp. 10–23, 01 2020.

[38] S. Eze and M. Oyesanya, "Fractional order on the impact of climate change with dominant earth's fluctuations," *Mathematics of Climate and Weather Forecasting*, vol. 5, no. 1, pp. 1–11, 2019.

[39] A. Din, F. M. Khan, Z. U. Khan, A. Yusuf, and T. Munir, "The mathematical study of climate change model under nonlocal fractional derivative," *Partial Differential Equations in Applied Mathematics*, vol. 5, 2022.

[40] I. Podlubny, *Fractional Differential Equations*. Academic Press, 1999.

[41] Y. Li, Y. Chen, and I. Podlubny, "Stability of fractional order nonlinear dynamic systems: Lyapunov direct method and generalized mittag-leffler stability," *Computers & Mathematics with Applications*, vol. 59, pp. 1810–1821, 2010.

[42] K. Diethelm, *The Analysis of Fractional Differential Equations*. Springer, 2010.

[43] K. Diethelm, "An algorithm for the numerical solution of differential equations of fractional order," *Electronic Transactions on Numerical Analysis*, vol. 5, 08 1998.

[44] K. Diethelm and N. J. Ford, "Analysis of fractional differential equations," *Journal of Mathematical Analysis and Applications*, vol. 265, no. 2, pp. 229–248, 2002.

[45] D. Kumarathunge *et al.*, "Acclimation and adaptation components of the temperature dependence of plant photosynthesis at the global scale," *New Phytologist*, vol. 222, 12 2018.

[46] C. Robinson, "Plankton gross production and respiration in the shallow water hydrothermal systems of Milos, Aegean Sea," *Journal of Plankton Research*, vol. 22, no. 5, pp. 887–906, 2000.

[47] K. Hancke and R. Glud, "Temperature effects on respiration and photosynthesis in three diatom-dominated benthic communities," *Aquatic Microbial Ecology*, vol. 37, no. 3, pp. 265–281, 2004.

[48] J. Hansen, R. Ruedy, M. Sato, and K. Lo, "Global surface temperature change," *Reviews of Geophysics*, vol. 48, no. 4, 2010.